pharmaceutics

MDPI

Article

COMPARATIVE ANALYSIS OF NEW CYANOARYLPORPHYRAZINE AND ITS IRON COMPLEX AS PHOTOSENSITIZERS FOR ANTICANCER PHOTODYNAMIC THERAPY

Lydia N. Shestakova [1], Tatyana S. Lyubova [2], Artyom O. Belotelov [1], Nina N. Peskova [1], Larisa G. Klapshina [2], Irina V. Balalaeva [1] and Natalia Yu. Shilyagina [1,*]

[1] Lobachevsky State University, Gagarin Ave., 23, Nizhny Novgorod, 603950, Russia
[2] Razuvaev Institute of Organometallic Chemistry, Russian Academy of Sciences, st. Tropinina, 49, Nizhny Novgorod, 603137, Russia
* Correspondence: nat-lekanova@yandex.ru

Citation: Shestakova, L.N; Lyubova, T.S.; Belotelov, A.O.; Peskova, N.N.; Klapshina, L.G.; Balalaeva, I.V.; Shilyagina, N.Yu. Comparative analysis of new cyanoarylporphyrazine and its iron complex as photosensitizers for anticancer photodynamic therapy. *Pharmaceutics* **2022**, *14*, x. https://doi.org/10.3390/xxxxx

Academic Editor: Firstname Lastname

Received: date
Accepted: date
Published: date

Publisher's Note: MDPI stays neutral with regard to jurisdictional claims in published maps and institutional affiliations.

Copyright: © 2022 by the authors. Submitted for possible open access publication under the terms and conditions of the Creative Commons Attribution (CC BY) license (https://creativecommons.org/licenses/by/4.0/).

Abstract: Photodynamic therapy (PDT) is a rapidly developing modality of primary and adjuvant anticancer treatment. A leading trend today is the search for new effective photodynamic agents. One of the approaches to the creation of successful photosensitizers is the development of targeted delivery systems with the function of controlling the release of the agent in the tumor. Previously, our research team synthesized and studied compounds from the cyanoporphyrazine group that are both photosensitizers and sensors of the local microenvironment. With their help, we demonstrated the possibility of assessing the release of photosensitizer from the transport carrier in real time *in vivo*. In this study we focus on a comparative study of the new tetra(2-naphthyl)tetracyanoporphyrazine and its iron complex. Current research has shown that iron notably impacts the photophysical properties of cyanoporphyrazine: in the presence of iron, the quantum yield of fluorescence and the photostability of porphyrazine increases. It has also shown that the iron cation significantly affects the photobiological characteristics. For instance, the photodynamic index of a metal complex is higher than that of a metal-free base, but the rate of its accumulation in cells is lower. In general, the developed compounds are found to be very promising for PDT, including the use of transport delivery systems, and can be recommended for further *in vivo* studies.

Keywords: photodynamic therapy, PDT photosensitizer, porphyrazine, iron complex, cyanoarylporphyrazines

1. Introduction

Photodynamic therapy was developed over forty years ago and is now widely used in treating various types of cancer. PDT is used as an independent treatment method as well as an adjuvant therapy modality along with traditional methods of tumor treatment such as chemotherapy, radiation therapy and surgery [1]. This therapeutic procedure involves administration of a photosensitive compound (a photosensitizer, a PS), which target cells absorb. After absorption, tumor cells are exposed to the visible light of the wavelength that corresponds to the peaks of the PS excitation spectrum [2]. The excited PS reacts with oxygen which leads to generation of reactive oxygen species (ROS) such as singlet oxygen, superoxide anion, peroxides, hydroxyl radical, hydroperoxide radical, etc. The generated ROS trigger oxidative reactions which lead to the death of tumor cells. [3]. The anticancer effect of PDT is based on three main mechanisms: direct photodynamic effect on tumor cells, damage to the blood vessels that feed the tumor, and a systemic immune response. [4,5].

The main efforts in the field of experimental PDT have been focused on the screening of potential PS with different chemical structures. In vitro and in vivo studies demonstrate that physico-chemical properties of PS affect significantly the processes of ~~Ps~~ localization and its photodynamic activity in cells and tumor tissue [6]. Tetrapyrroles, such as hematoporphyrins [7], porphyrins [8-10], chlorins [11-13] and bacteriochlorins [14], purpurins [15,16], porphyrazines (tetraazaporphyrins) [17-19] and others have been studied as ~~the main~~ potential PSs.

One of the approaches to the modification of a photosensitizer is ~~an approach~~ based on the inclusion of various metals in the center or peripheral environment of the macrocycle. The presence and nature of the central metal ion strongly influences the photochemical, photophysical, and photobiological properties of PS [20], such as water solubility, triplet state lifetime, intersystem crossing efficiency, quantum yield and fluorescence lifetime, photostability [21,22].

The most common metals used in the modification of tetrapyrrolic PSs are aluminum (Al), iron (Fe), zinc (Zn), copper (Cu), tin (Sn), manganese (Mn), nickel (Ni) [22], the less common metals are heavy metals such as ruthenium (Ru), iridium (Ir), platinum (Pt), lutetium (Lu), palladium (Pd), Rhodium (Rh), thulium (Tm), ytterbium (Yb) [23,24].

Although metal complexes of photosensitizers have been studied for a long time, only two of them have passed clinical trials. They are TOOKADS® soluble (Padeliporfin, WST11), which is a palladium-coordinated bacteriochlorophyll a, approved for the treatment of prostate cancer in Mexico, Israel and over 30 EU countries [25] and Photosens®, which is sulfonated aluminum phthalocyanine approved for the treatment of skin, liver, breast, lung and gastrointestinal cancer in Russia [26]. Several photosensitizer metal complexes are currently going through clinical trials: Purlytin® (Rostaporfin), a tin-coordinated phthalocyanine PS, which is in clinical trials in the USA for the treatment of basal cell carcinoma [27]; Antrin® (Motexafin Lutetium), a texaphyrin-based compound with a lutetium metal center and axially bound acetate ions for the treatment of prostate cancer, brain cancer, breast cancer, cervical cancer [28,29]; ruthenium polypyridine complex TLD-1433 clinically tested in Canada for invasive bladder cancer [30].

Another approach to improve PDT efficiency is the development of delivery systems for photosensitizers [31]. Nanosized carriers are of particular interest as such delivery systems. They have a number of advantages connected with maintenance of solubility, increase in time of circulation of PS in blood, an opportunity of the address delivery and controlled release of PS in an area of interest ~~and a number of other advantages~~ [32].

Previously, our research team described the novel group of tetracyanotetra(aryl)porphyrazines as prospective photosensitizers for PDT [33-36].The uniqueness of these compounds lies in the fact that they combine the properties of effective photodynamic agents and microenvironment sensors. [37,38].

In earlier work, we have shown that cyanoporphyrazines can be efficiently loaded and retained in nanoscale and submicron containers of different nature. ~~In the study [39]~~ showed how hydrophobic cyanoporphyrazine dyes are effectively loaded into liposomes of different lipid composition, which subsequently promotes their high uptake by tumor cells while preserving the photoinduced toxicity of porphyrazine. In the works [40] and [41] demonstrated for the first time that cyanoporphyrazines are successfully loaded into amphiphilic polymer brushes and, due to the presence of such a container, selectively accumulate and retain in tumors, providing subsequent successful photodynamic therapy. The potential of cyanoporphyrazines is most fully reflected ~~in [42], where~~ the release of photosensitizer from vaterite particles was first demonstrated in real time *in vivo*. This possibility appeared due to the unique property of porphyrazines - the dependence of the fluorescence lifetime on the microenvironment. The obtained results aroused interest in further modification and study of porphyrazines not only as potential agents for PDT, but also as sensors to assess the dynamics of drug release from the transport carrier.

In this study, we perform a detailed analysis of two novel photosensitizers namely tetra(2-naphthyl)tetracyanoporphyrazine (hereinafter, **PzNf**) and its iron complex (herei-

nafter, **FePzNf**) in order to assess their possible application in PDT and evaluate the effect of adding an iron metal atom in the center of the porphyrazine macrocycle. Herein, we present data on photophysical properties of the photosensitizers, including absorption and fluorescence spectra; fluorescence quantum yield in low and high viscosity media; and the dynamics of photobleaching and photodegradation quantum yield. In addition, we study cellular uptake and dark and photoinduced cytotoxicity of **PzNf** and **FePzNf** against human epidermoid carcinoma cells.

2. Materials and Methods

2.1. Photosensitizers

Two photoactive dyes have been tested: tetra(2-naphthyl)tetracyanoporphyrazine (hereinafter, **PzNf**) and its iron complex (hereinafter, **FePzNf**) (Figure1.). The synthesis of the former had been described previously [33,43] and the latter had been prepared by ferrous acetate mixing with free-base in inert atmosphere that is similarly to gadolinium cyanoarylporphyrazine complex that had been reported by us earlier [44].

2.2. Cell culture

The experiments were performed using human epidermoid carcinoma cells A431. The cells were cultured in 25 cm2 culture flasks (Corning, USA) at 37°C under 5% CO2 in Dulbecco's Modified Eagle Medium (DMEM, HyClone, USA) containing 2 mM L-glutamine (PanEco, Russia) and 10% fetal bovine serum (FBS, Thermo Fisher, USA). For passaging, the cells were carefully detached using a trypsin-versene solution (1:1) (PanEco, Russia).

2.3. Analysis of spectral properties and fluorescence quantum yield

To register the absorption and fluorescence spectra of **PzNf** and **FePzNf**, we used a Synergy MX plate reader (BioTek, USA). As a solvent, we used deionized water and glycerol, the concentration of PzNf and **FePzNf** in all studies was 5 μM. Absorption was recorded in the range of 300–700 nm, fluorescence was recorded in the range of 600–800 nm with excitation at a wavelength of 580 nm.

The quantum yield of fluorescence was determined relative to rhodamine B in ethanol ($\phi = 0.7$) [45]:

$$\varphi_1 = \frac{\varphi_0 \times F_0 \times D_0}{F_1 \times D_1} \quad (1),$$

where ϕ_0 is the quantum yield of rhodamine; ϕ_1 is the quantum yield of tested PS; F_1 and F_0 are the area under the fluorescence curve for the tested PS (**PzNf** or **FePzNf**) and rhodamine B, respectively; D_1 and D_0 are optical density of the PS and rhodamine B at the excitation wavelength.

2.4. Photobleaching

Photobleaching was analyzed for **PzNf** or **FePzNf** solutions in glycerol at a concentration of 5 μM. When evaluating photobleaching, the solutions were placed in the wells of a 96-well plate and irradiated with an LED light source for microplates (λex 615–635 nm, 20 mW/cm2) [46]. Registration of absorption spectra was carried out in the wavelength range of 450-700 nm before and after irradiation in various light doses. The measurements were taken using a Synergy MX plate reader. The experiment was carried out at a room temperature of 25 0C.

The photodegradation quantum yield was calculated using the following equation [47,48]:

$$\phi = \frac{\frac{D_0 - D}{D_0} \times C \times N_A \times V}{N_q} \quad (2),$$

where D_0 and D are optical density of PS before and after irradiation; C is the concentration of the photosensitizer before irradiation; N_A is the Avogadro number; V is the volume of the solution and N_q is the number of quanta absorbed by the solution.
N_q was defined as:

$$N_q = \frac{(1-10^{-D}) \times I \times \lambda \times t}{\hbar \times c} \quad (3),$$

where I is the radiation power density; λ is the wavelength of the irradiation light; t is the irradiation time in seconds; c is the speed of light; and h is Planck's constant.

2.5. Study of the dynamics of cellular uptake

The A431 cells were planted in a 96-well plate at 10 000 cells per well and cultured for 12 hours. Then, the medium was replaced with a fresh serum-free growth medium containing **PzNf** or **FePzNf** at a concentration of 5 μM. The accumulation of pophyazines by cells was studied using laser scanning fluorescence confocal microscopy. We used a scanning confocal microscope Axio Observer Z1 LSM 710 NLO/Duo (Carl Zeiss, Germany) equipped with C-Apochromat 63× water immersion objective lens with numerical aperture of 1.2. Fluorescence was recorded in the range of 600–750 nm with excitation at a wavelength of 594 nm. Image analysis was performed before and at various time points after adding **PzNf** and **FePzNf** to the cells. The obtained images were used to evaluate the fluorescence intensity of porphyrazines in the cell cytoplasm. For this, the ZEN 2012 software (Carl Zeiss, Germany) was used; about 10 cells per field of view were used for analysis.

To analyze the dynamics of cellular uptake, cells were planted in 96-well plates (Corning, USA) in the amount of 10 000 cells per well and cultured overnight until they were completely attached. Then the culture medium was replaced with a serum-free medium containing **PzNf** or **FePzNf** at a concentration of 5 μM, and the fluorescence intensity was recorded with a Synergy MX plate reader at a wavelength of 660 nm with excitation at 590 nm. The fluorescence signal was normalized to the maximum value recorded at the end of the incubation to eliminate the effect of cell culture density on the result.

2.6. Analysis of dark toxicity and photodynamic activity

The A431 cells were planted in a 96-well plate at a density of 4 000 cells per well and cultured for 12 hours. Then **PzNf** or **FePzNf** was added to the cells in a serum-free medium at a concentration range from 0.0001 to 100 μM and incubated for 4 hours. After that, the medium with porphyrazines was replaced with a complete culture medium.

To analyze photodynamic activity, cells were exposed to light at a dose of 20 J/cm^2 using a LED light source (λex 615–635 nm, 20 mW/cm^2) [46]. To analyze dark toxicity, the cells were incubated with **PzNf** or **FePzNf** in the dark under CO_2 incubator conditions for the same period of time. As a control group, we used cells that were incubated according to the same protocol, but without adding **PzNf** or **FePzNf**. The MTT test was carried out 24 hours after light exposure.

To do this, the medium in the plates was replaced with a serum-free fresh growth medium with 0.5 mg/mL of MTT-reagent and it was incubated for 4 hours. (Alfa Aesar, UK). After that, the medium was taken and dimethyl sulfoxide (DMSO, PanEco, Russia) was added, 200 μl per well, to dissolve the formed formazan crystals. The optical density of the resulting solutions at a wavelength of 570 nm was measured using a Synergy MX plate reader.

Based on the results, cell viability was analyzed after photodynamic exposure in relation to the optical density of the formazan solution in each well to the control group. The

resulting dose-effect relationships were used to calculate IC_{50}, the dose of the test substance leading to inhibition of cell culture growth by 50%. The results were processed using GraphPad Prism (v.9.0) (GraphPad Software, USA).

3. Results

Two ~~types of~~ photoactive dyes, tetra(2-naphthyl)tetracyanoporphyrazine (**PzNf**) and its iron complex (**FePzNf**) were studied (Figure 1). It should be noted that the cyanoporphyrazine iron complex was synthesized and studied for the first time.

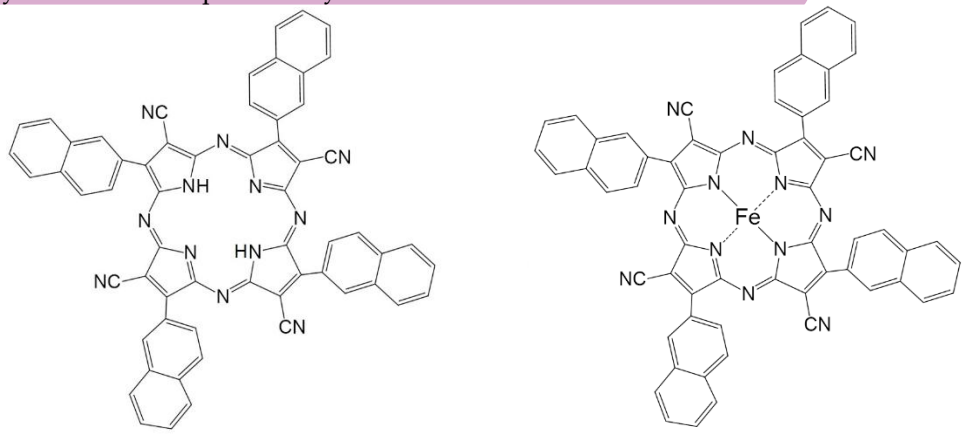

(**a**) (**b**)

Figure 1. Structures of **PzNf** (**a**) and **FePzNf** (**b**)

3.1. Spectral properties and fluorescence quantum yield of PzNf and FePzNf

The studied compounds belong to the cyanoporphyrazine group, for which the dependence of fluorescent properties, such as quantum yield and fluorescence lifetime, on the viscosity of the medium is shown [37]. Assuming the rotary properties of **PzNf** and **FePzNf**, we have studied the spectral properties in both water and glycerol. It should be noted that measurements in glycerin were carried out at a temperature of 25 ^{0}C, the viscosity of glycerol was 858.4 cP.

The analysis of photophysical properties of PSs has revealed that both porphyrazines absorb and fluoresce in the optical window in biological tissue 500-650 nm and 600-800 nm, respectively (Figure 2, Figure S1, Table 1).

We have registered an increase in the fluorescence intensity for PzNf and FePzNf in glycerol as compared to an aqueous solution, which confirms our assumption that the studied compounds belong to the class of fluorescent molecular rotors. Thus, the quantum yield of **PzNf** in glycerol increased 21.5 times compared to an aqueous solution, and 10.4 times for **FePzNf**. The presence of an iron atom led to an increase in the quantum yield of fluorescence both in water and in glycerol by 3 and 1.5 times, respectively (Table 1).

The presence of iron in the porphyrazine macrocycle has led to a bathochromic shift of the absorption peak by 20 nm when water was used as a solvent (Figure S1) while in glycerin, the position of the absorption maxima for **PzNf** and **FePzNf** was the same (Figure 2, Table 1). The addition of an iron atom has also led to a decrease in the molar extinction coefficient by a factor of 5 in water and by a factor of 2.6 in glycerol.

Moreover, the presence of iron has not affected the positions of fluorescence maxima both in water and glycerol. However, an increase in viscosity dissolved the shift of the fluorescence peak to the short wavelength region of the pigment. (Table 1). It should be noted that the fluorescence peak of the studied porphyrazines is quite wide compared to the "traditional" PSs, which is caused the peculiarities of their photophysical properties as fluorescent molecular rotors. They are characterized by the twisted intramolecular charge-transfer (TICT) state, which is accompanied by the formation of TICT-conformers

whose fluorescent signals are shifted to the long-wavelength region, which leads to a broadening of the fluorescence spectrum [49].

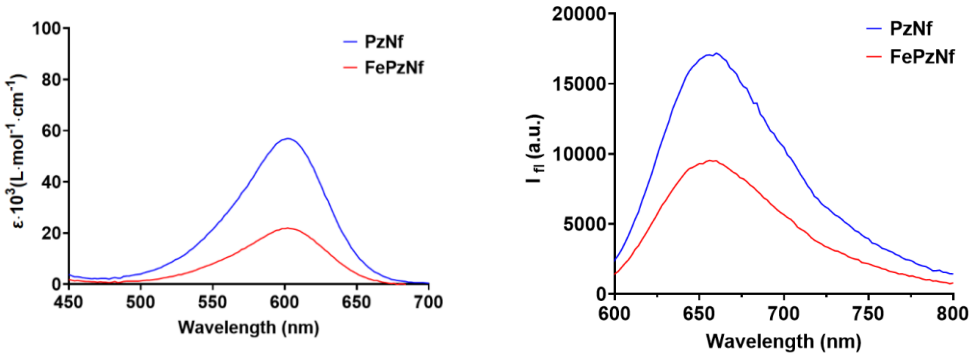

(**a**) (**b**)

Figure 2. Absorption (**a**) and fluorescence (**b**) spectra of **PzNf** and **FePzNf** in glycerin. ~~The fluorescence was excited at λ_{ex} 570 nm~~

Table 1. Spectral properties and fluorescence quantum yield of **PzNf** and **FePzNf**

Compound	**H_2O**				**Glycerin**			
	λ_{abs} (nm)	λ_{em} (nm)	ε, (L×mol^{-1}×cm^{-1})	ϕ (%)	λ_{abs} (nm)	λ_{em} (nm)	ε, (L×mol^{-1}×cm^{-1})	ϕ (%)
PzNf	590	675	1.2×10^5	0,6	600	660	5.7×10^4	12,9
FePzNf	610	675	2.4×10^4	1,8	600	656	2.2×10^4	18,7

3.2. Photobleaching of PzNf and FePzNf

The photodegradation quantum yield is an important parameter when calculating the dosage of a photosensitizer used in photodynamic therapy. The high photostability of the photosensitizer will avoid the use of high doses of the PS and reduce the radiation dose required to achieve a similar clinical result when using low-stability PSs [47].

To estimate the photobleaching coefficient of photosensitizers, we used a solution of PzNf and FePzNf in glycerin. Glycerol was used as a solvent in the assessment of photobleaching because of the photophysical features of the studied dyes. When energy is transferred to them in the form of a quantum of light, the resulting energy of the excited state can be spent through three main channels - intramolecular rotation, fluorescence, and intersystem conversion. In low-viscosity media, the priority channel for energy consumption is the rotation of separate parts of the molecule. The use of a relatively viscous medium reduces the contribution of the rotor movement and increases the contribution of other processes. It is important to note that such conditions are more relevant when modeling the behavior of the PS in the intracellular environment during the photodynamic reaction [37].

Both compounds demonstrated rather high photostability: at a dose of 100 J/cm2 the percentage of photobleaching was about 50%. The addition of an iron atom into the macrocycle led to an increase in the photostability of porphyrazine, so the photodegradation quantum yield reached 5.7×10-7 for PzNf and 4×10-7for FePzNf (Figure 3)

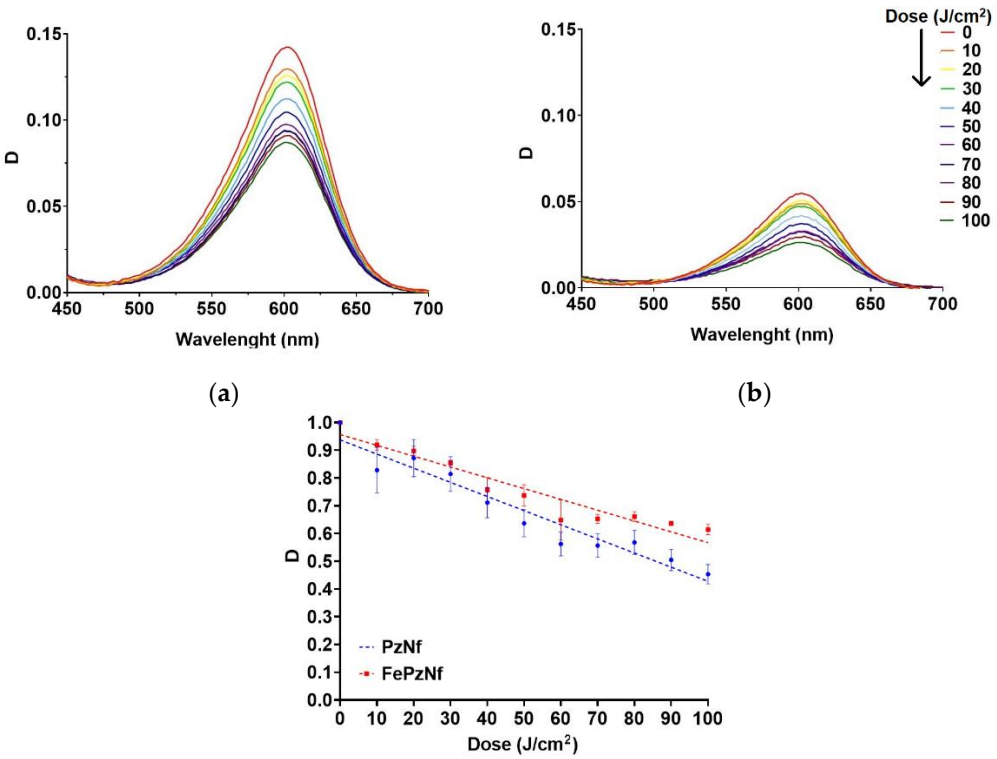

Figure 3. Photobleaching of **PzNf** and **FePzNf** in the glycerol solution under irradiation, **a** – photobleaching of **PzNf**; **b** – photobleaching of **FePzNf**; **c** – photobleaching of **PzNf** and **FePzNf** at maximum

3.3. Cellular uptake of PzNf and FePzNf

Photobiological properties of **PzNf** and **FePzNf** have been analyzed using human epidermoid carcinoma A431 cells. The choice of the cell line was determined by the fact that the PDT method is used to treat skin cancer [50,51]. Both photosensitizers were accumulated by cells, but with different dynamics: 15 minutes after adding the PSs to the incubation medium, the intensity of the fluorescence signal for **FePzNf** was 2.5 times lower compared to **PzNf**, but after 4 hours of incubation, the fluorescence signals almost leveled out, which allowed us to assume a difference in the cellular uptake rates of **PzNf** and **FePzNf** (Figure 4).

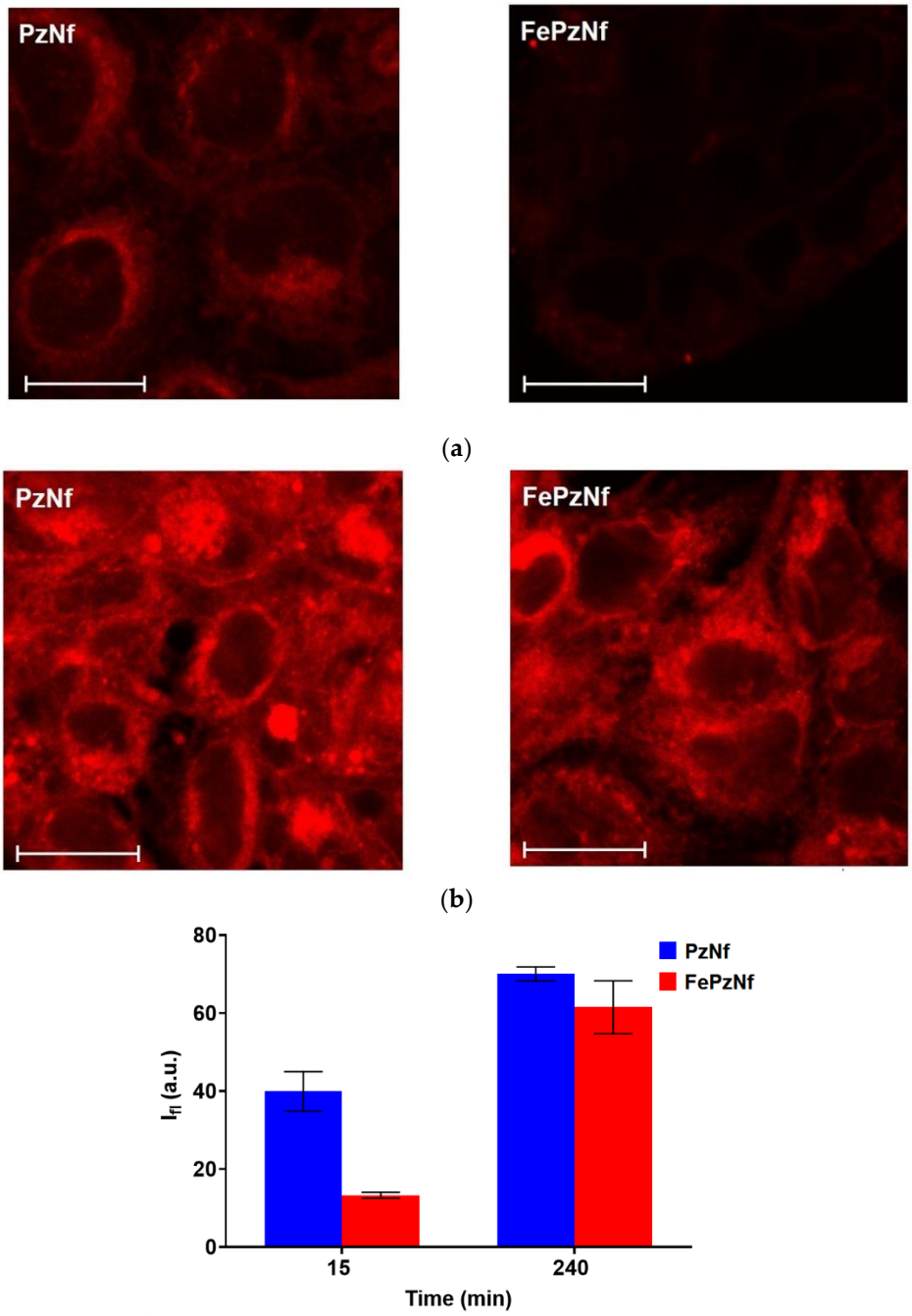

Figure 4. Analysis of the cellular uptake of **PzNf** and **FePzNf**. Representative confocal images of human epidermoid carcinoma A431 cells after 15 min (**a**) and 240 min (**b**) of incubation with **PzNf** and **FePzNf** (5 μM), minus the background signal not used 4 a.u. Relative accumulation of the **PzNf** and **FePzNf** after 15 and 240 min incubation estimated from a confocal microscopy experiment (**c**) (n ≥ 10). The data are presented as the mean values ± SD

To test the hypothesis about the difference in uptake rate for two compounds, we studied the accumulation dynamics of porphyrazines by spectrophotometry (Figure 5). It should be noted that the unique photophysical properties of the studied porphyrazines make it possible to use a measurement technique based on continuous recording of the cell fluorescence signal using a plate spectrofluorimeter. Porphyrazine added to the culture medium gives practically no fluorescence signal due to the low viscosity of the medium.

When porphyrazine enters a cell with a much higher viscosity, the fluorescent signal of porphyrazine increases and, therefore, we can record its accumulation in the cell at different time points without changing the medium.

It has been shown that the introduction of iron leads to a decrease in the rate of entry of porphyrazine into the cell: the maximum accumulation for **PzNf** was recorded already 1 hour after its addition to the incubation medium, while for **FePzNf** the maximum was reached after 4 hours (Figure 5). This may be caused by the interaction of iron with negatively charged groups of phospholipid bilayers. The results obtained confirm and explain the data recorded by laser scanning confocal microscopy.

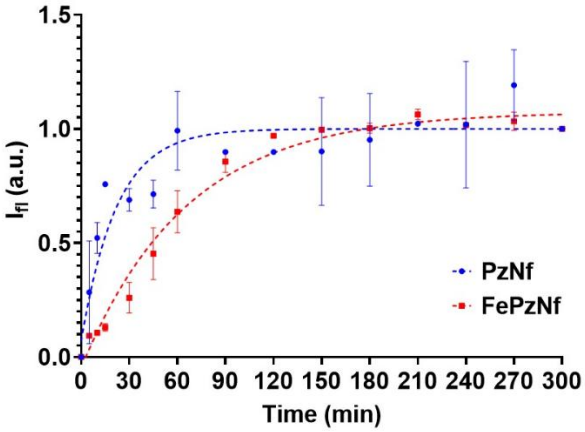

Figure 5. Dynamics of **PzNf** and **FePzNf** accumulation in human epidermoid adenocarcinoma A431 cells. The fluorescence signal was normalized to the maximum value recorded at the end of the incubation to eliminate the effect of cell culture density on the result. The data are presented as the mean values ± SD (n = 3)

3.4. Dark Toxicity and Photodynamic Activity of PzNf ~~u~~ FePzNf

We evaluated the toxic effects on the cell after 4 hours of incubation, when the accumulation maximum was recorded for **PzNf** and **FePzNf**. Under light irradiation, both compounds demonstrated photodynamic activity (~~Figure 4).~~ Adding an iron atom into the macrocycle leads to a twofold decrease in photodynamic activity – the IC_{50} value was 0.19 μM for **PzNf** and 0.4 μM for **FePzNf** (Table 2). However, for **FePzNf**, a decrease in dark toxicity by a factor of 3.5 was also observed (from 7 μM for **PzNf** to 24.18 μM for **FePzNf**, respectively), which results in the increase of the photodynamic index (the ratio of IC_{50} in the dark and under irradiation, IC_{50} dark/IC_{50} light). When adding iron, the photodynamic index almost doubled and reached a value of 60. Despite a slight decrease in photoinduced toxicity for **FePzNf**, an increase in the photodynamic index can potentially indicate a decrease in possible side effects on healthy organs and tissues and makes the iron complex quite interesting for follow-up study.

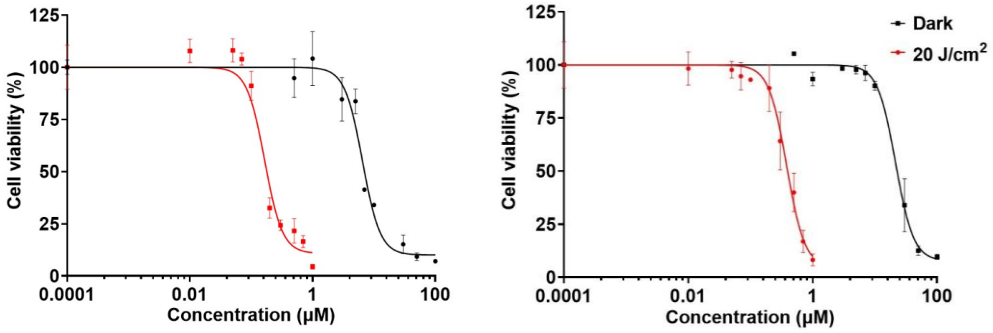

(**a**) (**b**)

Figure 6. Assessment of the dark toxicity and photodynamic activity of **PzNf** (**a**) and **FePzNf** (**b**) for human epidermoid carcinoma A431 cells. To induce a photodynamic response, the cells were irradiated with light 20 J/cm² (615–635 nm, 20 mW/cm²). The data are presented as the mean values ± SD (n = 3)

Table 2 Dark Toxicity and Photodynamic Activity of **PzNf** и **FePzNf** against A431 cells

Compound	*IC_{50} dark (μM)	*IC_{50} light (μM)	Photodynamic index
PzNf	7,04 (6,13 – 8,16)	0,19 (0,16 – 0,21)	37
FePzNf	24,18 (22,03 – 26,35)	0,4 (0,37 – 0,44)	60

* mean IC_{50} values and 95% confidence interval are indicated

4. Discussion

Photodynamic therapy is a fairly rapidly developing method of treating oncological diseases of various types and localizations. The PDT method is based on the use of photosensitizers that can selectively accumulate in pathological tissues. PS molecules absorb light of a certain wavelength and trigger reactions that lead to the death of target cells [1]. At one of the first stages in the development of PDT, the criteria for an ideal PS were formulated. An ideal photosensitizer should have the following properties: low dark and high light toxicity, high selectivity of accumulation in target cells and rapid elimination from healthy tissues, high quantum yield of generation of reactive oxygen species that cause death of target cells [52].

Furthermore, the current development strategy of the concept of an ideal PS is aimed at making PDT a more personalized therapeutic approach, as well as ensuring the activation of an antitumor immune response in addition to the elimination of cells of the primary tumor focus [53]

We have synthesized the novel group of porphyrazines as prospective photosensitizers for PDT [33-36]. The advantage of the investigated porphyrazines in comparison with the well-known clinically approved PSs lies in their additional modality to the photodynamic activity - the sensitivity of fluorescent properties to the viscous microenvironment. Porphyrazines belong to the class of molecular rotors, the photophysical properties (fluorescence quantum yield and lifetime) of which change significantly depending on the viscosity of the environment. In less viscous media, the excitation energy of porphyrazines is spent on intramolecular twisting or rotation of the side aryl groups, which leads to a very high nonradiative relaxation constant and, consequently, to a low fluorescence quantum yield and lifetime. In high-viscosity media, intramolecular rotation is difficult, and therefore there is a multiple increase in fluorescence quantum yield and lifetime. The high viscosity sensitivity of the photophysical properties of porphyrazines makes it possible to carry out dosimetric control of PDT and select treatment regimens for each patient [37,53].

Moreover, we have previously shown that some compounds from the group of porphyrazines are capable of inducing immunogenic cell death and can be used as effective photodynamic agents [19].

Our previous research indicates that porphyrazines are promising agents that can be used in personalized photodynamic therapy. Therefore, we continue to search for new promising compounds from this group with improved photophysical and photobiological properties.

In this article, we report on the study of metal complexes of porphyrazines for the first time. We have synthesized and analyzed the potential of tetra(2-naphthyl)tetracyanoporphyrazine (**PzNf**) and its iron complex (**FePzNf**) as novel photoactive dyes for PDT. We believe that the efficiency of PDT using FePzNf as a PS can be significantly increased by iron(II) cations reversibly bound to the macrocycle. Such an effect in the presence of iron can be expected as a result of the development of the Fenton reaction (the formation of hydroxide and hydroxyl radical by a reaction between Fe^{2+} and hydrogen peroxide) [53]. Our interest was also caused by recent publications on the role of iron-catalyzed enhancement of the antitumor effect due to the induction of ferroptosis as immunogenic cell death, which can effectively suppress tumor resistance to therapeutic effects [53,54]

PzNf and **FePzNf** absorb and fluoresce in the optical window in biological tissue 500-650 nm and 600-800 nm, respectively. The presence of iron does not affect the shape of the spectra and the position of the absorption and fluorescence maxima recorded at a wavelength of 600 and 660 nm, respectively. (Figure 2) In addition, we have registered an increase in the fluorescence quantum yield of **PzNf** and **FePzNf** in glycerol compared to an aqueous solution because this group of compounds belongs to the class of fluorescent molecular rotors.

Adding an iron cation has led to a decrease in the molar extinction coefficient by a factor of 5 in water and by a factor of 2.6 in glycerol. On the other hand, with iron, an increase in the fluorescence quantum yield by 3 and 1.5 times has been registered, in water and glycerol, respectively (Table 1). Iron has increased the photostability of porphyrazine, so the photobleaching quantum yield has reached 5.7×10^{-7} for **PzNf** and 4×10^{-7} for **FePzNf** (Figure 3).

A study performed on epidermoid carcinoma cells A431 has shown that **PzNf** and **FePzNf** are ~~infiltrated and~~ accumulated by tumor cells (Figure 4). The presence of iron in the macrocycle leads to a decrease in the rate of accumulation of porphyrazine which may be caused by the fact that iron interacts with negatively charged groups of phospholipid bilayers. This property can be of great importance for the pharmacokinetics of the drug in the *in vivo* system. Once in the blood, a PS is in two fractions: bound to plasma proteins or high- and low-density lipoproteins or bound to cellular components of the blood. Protein binding reduces PS diffusion into cells and tissues, while binding to intracellular components increases it, thereby reduces the toxic load on non-target organs and tissues.

The analysis of photodynamic activity has shown that adding an iron atom into the macrocycle leads to a twofold decrease in photodynamic activity (Table 2). However, for **FePzNf**, a 3.5-fold decrease in dark toxicity is observed, which ultimately leads to an increase in the photodynamic index, which almost doubles compared to the free base and reaches a value of 60. The results obtained in this study play an important role for clinical PDT, since a high photodynamic index may potentially indicate a decrease in possible side effects on healthy organs and tissues.

To sum up, our studies reveal that **PzNf** and **FePzNf** could be considered as potent agents for PDT with perspective photophysical and photbiological properties.

5. Conclusions

We have synthesized two photo-active dyes of the tetracyanotetra(aryl)porphyrazine group, **PzNf** and **FePzNf**, and studied their photophysical and photobiological properties as well as the influence of iron as a central cation in the porphyrazine macrocycle. The re-

sulting compounds have spectral properties suitable for PDT. In particular, they are characterized by absorption and fluorescence in the region of the "biological transparency window" of tissues and are characterized by the sensitivity of fluorescent properties to the viscosity of the medium. We have shown that iron has a significant effect on the photophysical properties of cyanoporphyrazine: in the presence of iron, the quantum yield of fluorescence and the photostability of porphyrazine increases. A study conducted on epidermoid carcinoma cells has shown that **PzNf** and **FePzNf** penetrate tumor cells and are accumulate by these cells, while the presence of an iron atom leads to a decrease in the rate of accumulation of the compound by cells, which may be related to the fact that iron interacts with negatively charged groups of phospholipid bilayers. This feature of **FePzNf** may be of further importance for the pharmacokinetics of the compound in *in vivo* experiments. The compounds show high photodynamic activity against tumor cells *in vitro*. In addition, the presence of the iron cation lead to an increase in the photodynamic index and a decrease in dark toxicity, which could potentially indicate a decrease in side effects for healthy organs and tissues at the level of the whole organism. In general, both compounds are promising for PDT and can be recommended for further *in vivo* studies.

Supplementary Materials:

Author Contributions: Conceptualization, Larisa Klapshina, Irina Balalaeva and Natalia Shilyagina; Investigation, Lydia Shestakova and Natalia Shilyagina; Methodology, Lydia Shestakova, Tatyana Lyubova, Artyom Belotelov and Nina Peskova; Visualization, Lydia Shestakova and Artyom Belotelov; Writing – review & editing, Lydia Shestakova and Natalia Shilyagina.

Funding: The research was carried out in Research scientific laboratory of "Chemistry of natural products and their synthetic analogues" of Scientific Educational Centre "Technoplatform 2035".

N.Yu.S. thanks for the personal support in the form of a grant from the President of the Russian Federation for young scientists and graduate students (SP1609.2021.4) for synthesizing and studying photophysical properties of PzNf and FePzNf.

N.N.P. thanks for the personal support in the form of a grant from the President of the Russian Federation for young scientists and graduate students (SP2067.2021.4) for studying photobiological properties of PzNf and FePzNf.

Institutional Review Board Statement: Not applicable.

Informed Consent Statement: Not applicable

Data Availability Statement: Not applicable

Conflicts of Interest: The authors have no conflicts of interest to declare

References

1. Kwiatkowski, S.; Knap, B.; Przystupski, D.; Saczko, J.; Kędzierska, E.; Knap-Czop, K.; Kotlińska, J.; Michel, O.; Kotowski, K.; Kulbacka, J. Photodynamic therapy – mechanisms, photosensitizers and combinations. *Biomedicine & Pharmacotherapy* **2018**, *106*, 1098-1107, doi:https://doi.org/10.1016/j.biopha.2018.07.049.
2. Dobson, J.; de Queiroz, G.F.; Golding, J.P. Photodynamic therapy and diagnosis: Principles and comparative aspects. *The Veterinary Journal* **2018**, *233*, 8-18, doi:https://doi.org/10.1016/j.tvjl.2017.11.012.
3. Hamblin, M.R. Photodynamic Therapy for Cancer: What's Past is Prologue. *Photochem Photobiol* **2020**, *96*, 506-516.
4. Agostinis, P.; Berg, K.; Cengel, K.A.; Foster, T.H.; Girotti, A.W.; Gollnick, S.O.; Hahn, S.M.; Hamblin, M.R.; Juzeniene, A.; Kessel, D.; et al. Photodynamic therapy of cancer: an update. *CA Cancer J Clin* **2011**, *61*, 250-281.
5. Alzeibak, R.; Mishchenko, T.A.; Shilyagina, N.Y.; Balalaeva, I.V.; Vedunova, M.V.; Krysko, D.V. Targeting immunogenic cancer cell death by photodynamic therapy: past, present and future. *Journal for ImmunoTherapy of Cancer* **2021**, *9*, e001926, doi:10.1136/jitc-2020-001926.
6. Castano, A.P.; Demidova, T.N.; Hamblin, M.R. Mechanisms in photodynamic therapy: part one—photosensitizers, photochemistry and cellular localization. *Photodiagnosis and Photodynamic Therapy* **2004**, *1*, 279-293, doi:https://doi.org/10.1016/S1572-1000(05)00007-4.

7. Li, M.-Y.; Gao, Y.-H.; Zhang, J.-H.; Mi, L.; Zhu, X.-X.; Wang, F.; Zhou, X.-P.; Yan, Y.-J.; Chen, Z.-L. Synthesis and evaluation of novel fluorinated hematoporphyrin ether derivatives for photodynamic therapy. *Bioorganic Chemistry* **2021**, *107*, 104528, doi:https://doi.org/10.1016/j.bioorg.2020.104528.
8. Gomes, A.; Neves, M.; Cavaleiro, J.A.S. Cancer, Photodynamic Therapy and Porphyrin-Type Derivatives. *An Acad Bras Cienc* **2018**, *90*, 993-1026.
9. Amos-Tautua, B.M.; Songca, S.P.; Oluwafemi, O.S. Application of Porphyrins in Antibacterial Photodynamic Therapy. *Molecules* **2019**, *24*, doi:10.3390/molecules24132456.
10. Zhang, Z.; Yu, H.J.; Wu, S.; Huang, H.; Si, L.P.; Liu, H.Y.; Shi, L.; Zhang, H.T. Synthesis, characterization, and photodynamic therapy activity of 5,10,15,20-Tetrakis(carboxyl)porphyrin. *Bioorg Med Chem* **2019**, *27*, 2598-2608.
11. Otvagin, V.F.; Kuzmina, N.S.; Krylova, L.V.; Volovetsky, A.B.; Nyuchev, A.V.; Gavryushin, A.E.; Meshkov, I.N.; Gorbunova, Y.G.; Romanenko, Y.V.; Koifman, O.I.; et al. Water-Soluble Chlorin/Arylaminoquinazoline Conjugate for Photodynamic and Targeted Therapy. *Journal of Medicinal Chemistry* **2019**, *62*, 11182-11193, doi:10.1021/acs.jmedchem.9b01294.
12. Otvagin, V.F.; Nyuchev, A.V.; Kuzmina, N.S.; Grishin, I.D.; Gavryushin, A.E.; Romanenko, Y.V.; Koifman, O.I.; Belykh, D.V.; Peskova, N.N.; Shilyagina, N.Y.; et al. Synthesis and biological evaluation of new water-soluble photoactive chlorin conjugate for targeted delivery. *European Journal of Medicinal Chemistry* **2018**, *144*, 740-750, doi:https://doi.org/10.1016/j.ejmech.2017.12.062.
13. Mal'shakova, M.V.; Pylina, Y.I.; Belykh, D.V. Novel hydrophilic galactose-conjugated chlorin e(6) derivatives for photodynamic therapy and fluorescence imaging. *Bioorg Med Chem Lett* **2019**, *29*, 2064-2069.
14. Pratavieira, S.; Uliana, M.P.; dos Santos Lopes, N.S.; Donatoni, M.C.; Linares, D.R.; de Freitas Anibal, F.; de Oliveira, K.T.; Kurachi, C.; de Souza, C.W.O. Photodynamic therapy with a new bacteriochlorin derivative: Characterization and in vitro studies. *Photodiagnosis and Photodynamic Therapy* **2021**, *34*, 102251, doi:https://doi.org/10.1016/j.pdpdt.2021.102251.
15. Zhang, D.; Feng, F.; Li, Q.; Wang, X.; Yao, L. Nanopurpurin-based photodynamic therapy destructs extracellular matrix against intractable tumor metastasis. *Biomaterials* **2018**, *173*, 22-33, doi:https://doi.org/10.1016/j.biomaterials.2018.04.045.
16. Singh, J.; Hussain, Y.; Luqman, S.; Meena, A. Purpurin: A natural anthraquinone with multifaceted pharmacological activities. *Phytotherapy Research* **2021**, *35*, 2418-2428, doi:https://doi.org/10.1002/ptr.6965.
17. Mishchenko, T.A.; Turubanova, V.D.; Mitroshina, E.V.; Alzeibak, R.; Peskova, N.N.; Lermontova, S.A.; Klapshina, L.G.; Balalaeva, I.V.; Vedunova, M.V.; Krysko, D.V. Effect of novel porphyrazine photosensitizers on normal and tumor brain cells. *Journal of Biophotonics* **2020**, *13*, e201960077, doi:https://doi.org/10.1002/jbio.201960077.
18. Balalaeva, I.V.; Mishchenko, T.A.; Turubanova, V.D.; Peskova, N.N.; Shilyagina, N.Y.; Plekhanov, V.I.; Lermontova, S.A.; Klapshina, L.G.; Vedunova, M.V.; Krysko, D.V. Cyanoarylporphyrazines with High Viscosity Sensitivity: A Step towards Dosimetry-Assisted Photodynamic Cancer Treatment. *Molecules* **2021**, *26*, 5816.
19. Turubanova, V.D.; Mishchenko, T.A.; Balalaeva, I.V.; Efimova, I.; Peskova, N.N.; Klapshina, L.G.; Lermontova, S.A.; Bachert, C.; Krysko, O.; Vedunova, M.V.; et al. Novel porphyrazine-based photodynamic anti-cancer therapy induces immunogenic cell death. *Scientific Reports* **2021**, *11*, 7205, doi:10.1038/s41598-021-86354-4.
20. Wu, Y.; Li, S.; Chen, Y.; He, W.; Guo, Z. Recent advances in noble metal complex based photodynamic therapy. *Chemical Science* **2022**, *13*, 5085-5106, doi:10.1039/d1sc05478c.
21. Ali, H.; van Lier, J.E. Metal complexes as photo- and radiosensitizers. *Chem Rev* **1999**, *99*, 2379-2450.
22. Josefsen, L.B.; Boyle, R.W. Photodynamic Therapy and the Development of Metal-Based Photosensitisers. *Metal-Based Drugs* **2008**, *2008*, 276109, doi:10.1155/2008/276109.
23. Li, J.; Chen, T. Transition metal complexes as photosensitizers for integrated cancer theranostic applications. *Coordination Chemistry Reviews* **2020**, *418*, 213355, doi:https://doi.org/10.1016/j.ccr.2020.213355.
24. Tuhl, A.; Makhseed, S.; Zimcik, P.; Al-Awadi, N.; Novakova, V.; Samuel, J. Heavy metal effects on physicochemical properties of non-aggregated azaphthalocyanine derivatives. *Journal of Porphyrins and Phthalocyanines* **2012**, *16*, 817-825, doi:10.1142/s1088424612500800.
25. Weersink, R.A.; Bogaards, A.; Gertner, M.; Davidson, S.R.H.; Zhang, K.; Netchev, G.; Trachtenberg, J.; Wilson, B.C. Techniques for delivery and monitoring of TOOKAD (WST09)-mediated photodynamic therapy of the

prostate: Clinical experience and practicalities. *Journal of Photochemistry and Photobiology B: Biology* **2005**, *79*, 211-222, doi:https://doi.org/10.1016/j.jphotobiol.2005.01.008.

26. Sokolov, V.; Chissov, V.; Yakubovskaya, R.; Aristarkhova, E.; Filonenko, E.; Belous, T.; Vorozhtsov, G.; Zharkova, N.; Smirnov, V.; Zhitkova, M. *Photodynamic therapy (PDT) of malignant tumors by photosensitzer photosens: results of 45 clinical cases*; SPIE: 1996; Volume 2625.
27. Mang, T.S.; Allison, R.; Hewson, G.; Snider, W.; Moskowitz, R. A phase II/III clinical study of tin ethyl etiopurpurin (Purlytin)-induced photodynamic therapy for the treatment of recurrent cutaneous metastatic breast cancer. *Cancer J Sci Am* **1998**, *4*, 378-384.
28. Patel, H.; Mick, R.; Finlay, J.; Zhu, T.C.; Rickter, E.; Cengel, K.A.; Malkowicz, S.B.; Hahn, S.M.; Busch, T.M. Motexafin lutetium-photodynamic therapy of prostate cancer: short- and long-term effects on prostate-specific antigen. *Clin Cancer Res* **2008**, *14*, 4869-4876.
29. Finlay, J.C.; Zhu, T.C.; Dimofte, A.; Stripp, D.; Malkowicz, S.B.; Whittington, R.; Miles, J.; Glatstein, E.; Hahn, S.M. In vivo determination of the absorption and scattering spectra of the human prostate during photodynamic therapy. *Proc SPIE Int Soc Opt Eng* **2014**, *14*, 132-142.
30. Monro, S.; Colón, K.L.; Yin, H.; Roque, J.; Konda, P.; Gujar, S.; Thummel, R.P.; Lilge, L.; Cameron, C.G.; McFarland, S.A. Transition Metal Complexes and Photodynamic Therapy from a Tumor-Centered Approach: Challenges, Opportunities, and Highlights from the Development of TLD1433. *Chemical Reviews* **2019**, *119*, 797-828, doi:10.1021/acs.chemrev.8b00211.
31. Hoffman, A.S. The origins and evolution of "controlled" drug delivery systems. *J Control Release* **2008**, *132*, 153-163.
32. Yu, X.T.; Sui, S.Y.; He, Y.X.; Yu, C.H.; Peng, Q. Nanomaterials-based photosensitizers and delivery systems for photodynamic cancer therapy. *Biomater Adv* **2022**, *135*, 22.
33. Lermontova, S.; Grigoryev, I.; Peskova, N.; Ladilina, E.; Lyubova, T.; Plekhanov, V.; Grishin, I.; Balalaeva, I.; Klapshina, L. Cyano-Aryl Porphyrazine Pigments with Polycyclic Substituents as the Promising Agents for Photodynamic Therapy and Potential Sensors of Local Viscosity. *Macroheterocycles* **2019**, *12*, 268-275, doi:10.6060/mhc190865k.
34. Lermontova, S.A.; Grigor'ev, I.S.; Ladilina, E.Y.; Balalaeva, I.V.; Shilyagina, N.Y.; Klapshina, L.G. Porphyrazine Structures with Electron-Withdrawing Substituents as the Base for Materials for Photonics and Biomedicine. *Russian Journal of Coordination Chemistry* **2018**, *44*, 301-315, doi:10.1134/s1070328418040061.
35. Lermontova, S.A.; Grigoryev, I.S.; Shilyagina, N.Y.; Peskova, N.N.; Balalaeva, I.V.; Shirmanova, M.V.; Klapshina, L.G. New porphyrazine macrocycles with high viscosity-sensitive fluorescence parameters. *Russian Journal of General Chemistry* **2016**, *86*, 1330-1338, doi:10.1134/s1070363216060189.
36. Lermontova, S.A.; Lyubova, T.S.; Ladilina, E.Y.; Plekhanov, V.I.; Balalaeva, I.V.; Boyarskii, V.P.; Klapshina, L.G. New Cyanoarylporphyrazines with High Sensitivity of Photophysical Parameters to Viscosity as Promising Agents for Photodynamic Therapy. *Russian Journal of General Chemistry* **2020**, *90*, 249-256, doi:10.1134/s1070363220020140.
37. Izquierdo, M.A.; Vyšniauskas, A.; Lermontova, S.A.; Grigoryev, I.S.; Shilyagina, N.Y.; Balalaeva, I.V.; Klapshina, L.G.; Kuimova, M.K. Dual use of porphyrazines as sensitizers and viscosity markers in photodynamic therapy. *Journal of Materials Chemistry B* **2015**, *3*, 1089-1096, doi:10.1039/c4tb01678e.
38. Krasnopeeva, E.L.; Melenevskaya, E.Y.; Klapshina, L.G.; Shilyagina, N.Y.; Balalaeva, I.V.; Smirnov, N.N.; Smirnov, M.A.; Yakimansky, A.V. Poly(methacrylic Acid)-Cellulose Brushes as Anticancer Porphyrazine Carrier. *Nanomaterials* **2021**, *11*, 1997.
39. Yudintsev, A.V.; Shilyagina, N.Y.; Dyakova, D.V.; Lermontova, S.A.; Klapshina, L.G.; Guryev, E.L.; Balalaeva, I.V.; Vodeneev, V.A. Liposomal Form of Tetra(Aryl)Tetracyanoporphyrazine: Physical Properties and Photodynamic Activity In Vitro. *J Fluoresc* **2018**, *28*, 513-522.
40. Shilyagina, N.Y.; Peskova, N.N.; Lermontova, S.A.; Brilkina, A.A.; Vodeneev, V.A.; Yakimansky, A.V.; Klapshina, L.G.; Balalaeva, I.V. Effective delivery of porphyrazine photosensitizers to cancer cells by polymer brush nanocontainers. *J Biophotonics* **2017**, *10*, 1189-1197.
41. Krasnopeeva, E.L.; Melenevskaya, E.Y.; Klapshina, L.G.; Shilyagina, N.Y.; Balalaeva, I.V.; Smirnov, N.N.; Smirnov, M.A.; Yakimansky, A.V. Poly(methacrylic Acid)-Cellulose Brushes as Anticancer Porphyrazine Carrier. *Nanomaterials* **2021**, *11*.

42. Parakhonskiy, B.V.; Shilyagina, N.Y.; Gusliakova, O.I.; Volovetskiy, A.B.; Kostyuk, A.B.; Balalaeva, I.V.; Klapshina, L.G.; Lermontova, S.A.; Tolmachev, V.; Orlova, A.; et al. A method of drug delivery to tumors based on rapidly biodegradable drug-loaded containers. *Applied Materials Today* **2021**, *25*, 101199, doi:https://doi.org/10.1016/j.apmt.2021.101199.
43. Klapshina, L.G.; Grigoryev, I.S.; Douglas, W.E.; Trifonov, A.A.; Gudilenkov, I.D.; Semenov, V.V.; Bushuk, B.A.; Bushuk, S.B. Metal template assembly of highly functionalized octacyanoporphyrazine framework from TCNE structural units. *Chemical Communications* **2007**, 1942-1944, doi:10.1039/b701994g.
44. Yuzhakova, D.V.; Lermontova, S.A.; Grigoryev, I.S.; Muravieva, M.S.; Gavrina, A.I.; Shirmanova, M.V.; Balalaeva, I.V.; Klapshina, L.G.; Zagaynova, E.V. In vivo multimodal tumor imaging and photodynamic therapy with novel theranostic agents based on the porphyrazine framework-chelated gadolinium (III) cation. *Biochim Biophys Acta Gen Subj* **2017**, *12*, 13.
45. Kubin, R.F.; Fletcher, A.N. Fluorescence quantum yields of some rhodamine dyes. *Journal of Luminescence* **1982**, *27*, 455-462, doi:https://doi.org/10.1016/0022-2313(82)90045-X.
46. Shilyagina, N.Y.; Plekhanov, V.; Shkunov, I.V.; Shilyagin, P.A.; Dubasova, L.V.; Brilkina, A.A.; Sokolova, E.A.; Turchin, I.V.; Balalaeva, I.V. LED Light Source for in vitro Study of Photosensitizing Agents for Photodynamic Therapy. **2014**, *6*, 15-22.
47. Hadjur, C.; Lange, N.; Rebstein, J.; Monnier, P.; van den Bergh, H.; Wagnières, G. Spectroscopic studies of photobleaching and photoproduct formation of meta(tetrahydroxyphenyl)chlorin (m-THPC) used in photodynamic therapy. The production of singlet oxygen by m-THPC. *Journal of Photochemistry and Photobiology B: Biology* **1998**, *45*, 170-178, doi:https://doi.org/10.1016/S1011-1344(98)00177-8.
48. Dadeko, A.V.; Lilge, L.; Kaspler, P.; Murav'eva, T.D.; Starodubtcev, A.M.; Kiselev, V.M.; Zarubaev, V.V.; Ponomarev, G.V. Photophysical properties and in vitro photocytotoxicity of disodium salt 2.4-di(alpha-methoxyethyl)-deuteroporphyrin-IX (Dimegine). *Photodiagnosis Photodyn Ther* **2019**, *25*, 35-42.
49. Haidekker, M.A.; Theodorakis, E.A. Molecular rotors—fluorescent biosensors for viscosity and flow. *Organic & Biomolecular Chemistry* **2007**, *5*, 1669-1678, doi:10.1039/b618415d.
50. Sidoroff, A.; Thaler, P. Taking treatment decisions in non-melanoma skin cancer—The place for topical photodynamic therapy (PDT). *Photodiagnosis and Photodynamic Therapy* **2010**, *7*, 24-32, doi:https://doi.org/10.1016/j.pdpdt.2009.12.004.
51. Griffin, L.L.; Lear, J.T. Photodynamic Therapy and Non-Melanoma Skin Cancer. *Cancers* **2016**, *8*, 98.
52. Xiao, Q.; Wu, J.; Pang, X.; Jiang, Y.; Wang, P.; Leung, A.W.; Gao, L.; Jiang, S.; Xu, C. Discovery and Development of Natural Products and their Derivatives as Photosensitizers for Photodynamic Therapy. *Curr Med Chem* **2018**, *25*, 839-860.
53. Mishchenko, T.A.; Balalaeva, I.V.; Vedunova, M.V.; Krysko, D.V. Ferroptosis and Photodynamic Therapy Synergism: Enhancing Anticancer Treatment. *Trends Cancer* **2021**, *7*, 484-487.
54. Ruiz-de-Angulo, A.; Bilbao-Asensio, M.; Cronin, J.; Evans, S.J.; Clift, M.J.D.; Llop, J.; Feiner, I.V.J.; Beadman, R.; Bascarán, K.Z.; Mareque-Rivas, J.C. Chemically Programmed Vaccines: Iron Catalysis in Nanoparticles Enhances Combination Immunotherapy and Immunotherapy-Promoted Tumor Ferroptosis. *iScience* **2020**, *23*, 101499, doi:https://doi.org/10.1016/j.isci.2020.101499.